Noninvasive Functional Brain Mapping by Change-Distribution Analysis of Averaged PET Images of $H_2{}^{15}O$ Tissue Activity

Peter T. Fox and Mark A. Mintun

Department of Neurology and Neurosurgery (Neurology), The Mallinckrodt Institute of Radiology, The McDonnell Center for Studies of Higher Brain Function, Washington University School of Medicine, St. Louis, Missouri

Change-distribution analysis and intersubject averaging of subtracted positron emission tomography (PET) images are new techniques for detecting, localizing, and quantifying state-dependent focal transients in neuronal activity. We previously described their application to cerebral blood flow images (intravenous bolus $H_2{}^{15}O$, Kety autoradiographic model). We now describe their application to images of $H_2{}^{15}O$ regional tissue activity without conversion to units of blood flow. The sensitivity and specificity of response detection and the accuracy of response localization were virtually identical for the two types of images. Response magnitude expressed in percent change from rest was slightly, but consistently smaller in tissue-activity images. Response magnitude expressed in z-score was the same for the two-image types. Most research and clinical applications of functional brain mapping can employ images of $H_2{}^{15}O$ tissue activity (intravenous bolus, 40-sec nondynamic scan) without conversion to units of blood flow. This eliminates arterial blood sampling, thereby simplifying and minimizing the invasivity of the PET procedure.

J Nucl Med 30:141–149, 1989

Mapping the functional organization of the human brain is an important and growing area of positron emission tomography (PET) that has clinical as well as research applications. Detailed maps of the sensory, motor, and cognitive operations of normal subjects, plotted in a standardized, stereotactic coordinate space, are accumulating rapidly (*1–5*). Preoperative clinical mapping of brain areas supporting speech, movement, and sensation is now possible (*3–6*). Moreover, behavioral activation can be used to study functional capacity and functional recovery following brain injury, providing information potentially of use in prognostication and rehabilitation (*3,7–9*).

Measurement of regional cerebral blood flow (rCBF) has proven a sensitive, simple, and versatile approach to functional brain mapping. Local CBF increases during transient neuronal activity are equal to (*10*) or greater than (*11,12*) the increases observed in glucose metabolic rate. Increases in oxygen metabolic rate during neuronal activation are minimal (*10,13*). Additionally, the extremely short scan duration (40 sec) and interscan interval (10 min) possible with bolus $H_2{}^{15}O$ (Kety autoradiographic model) are optimal for mapping. Uniform performance, even of very effortful tasks, is greatly facilitated by the brevity (40 sec) of the measurement. (We have successfully mapped language function in patients as young as 12 years of age). Obtaining multiple behavioral conditions in rapid succession permits image analysis based on intrasubject subtraction (task minus control), necessary for accurate response localization (*14*).

We have recently described two techniques for analysis of subtraction images (*15*). The first of these, change-distribution analysis, reduces an image of regional CBF change ($rCBF^{\Delta}$) to a distribution of change foci, each described by a location (x,y,z coordinate) and a magnitude. Physiological responses are identified by a signal-to-noise analysis that differentiates statistically significant outliers from background image noise by intensity. This analysis is entirely automated, making it both objective and efficient. Of particular value for clinical applications, statistical significance can be determined even for individual subjects.

Received Apr. 18, 1988; revision accepted Aug. 31, 1988.

For reprints contact: Peter T. Fox, MD, Div. of Radiation Sciences, Mallinckrodt Institute of Radiology, 510 S. Kingshighway, St. Louis, MO 63110.

The second technique is averaging $rCBF^{\Delta}$ images. In the $rCBF^{\Delta}$ image, responses appear as discrete foci of activity within a background of low-level, spatially random noise. Averaging images either between subjects (using a standardized stereotactic coordinate space) or within subject suppresses background noise and improves signal-to-noise ratio.

Change-distribution analysis and subtraction-image averaging are unaffected by simple scalar transformations (*15*). Yet, for the range of rCBF observed in the human, rCBF and regional $H_2{}^{15}O$ tissue activity (rA) are nearly linearly related (*16,17*). This suggests that functional brain mapping, using bolus, intravenous $H_2{}^{15}O$ and these image-analysis strategies, should be as sensitive and accurate for rA as for rCBF images. To test this, we applied these techniques to $H_2{}^{15}O$ images before (rA) and after (rCBF) application of the Kety autoradiographic model.

METHODS

All methods and materials were identical to those of our initial description of change-distribution analysis (*15*) with the exception that both rA and rCBF images were analyzed.

Tomograph Characteristics

The PETT VI system was employed in the low-resolution mode, simultaneously acquiring seven parallel slices with a center-to-center distance of 14.4 mm (*18*). Images were reconstructed by filtered backprojection to a resolution of 18 mm full width at half maximum (FWHM) and a pixel size of 2.7 mm by 2.7 mm.

Subject Preparation

Subjects were normal volunteers between the ages of 18 and 45 yr. Informed consent was obtained from each subject using forms and procedures approved for this study by the Human Studies and Radioactive Drug Research Committees of Washington University.

Subjects' heads were immobilized within a closely fitted, thermally molded, plastic facial mask individually made for each subject. After the mask cooled and became rigid (2–3 min), head alignment and planes of section were recorded with a lateral radiograph (*19*). Venous and arterial catheters were placed in opposite arms.

Tracer Techniques

Brain blood flow was measured using an adaptation of the Kety autoradiographic method (*16,20,21*). Water labeled with oxygen-15 (half-life, 123 sec) served as an inert, diffusible blood flow tracer and was administered as an intravenous bolus of 8–10 ml of saline containing 50–80 mCi. A 40-sec scan was initiated when the tracer bolus entered the brain, as indicated by an abrupt rise in the coincidence-counting rate of the tomograph. Arterial blood samples were obtained every 3–5 sec from isotope injection until scan completion, to provide an arterial time-radioactivity curve.

Behavioral States

Image noise was assessed using $rCBF^{\Delta}$ and rA^{Δ} images formed by the subtraction of intrasubject pairs of control-state images. The control state was eyes-closed rest. Twenty-one pairs were available, with interscan intervals ranging from 18–40 min.

Response stability was assessed using $rCBF^{\Delta}$ and rA^{Δ} images formed by intrasubject subtraction of a control-state image from a stimulated-state image (Fig. 1). The stimulus employed was vibration (130 Hz, 2 mm amplitude) of the fingers of the left hand (*3,11,13*). Twenty-eight stimulus-control pairs of images were available with interscan intervals ranging from 10 to 40 min.

For both behavioral states the subject's eyes were closed and room lights darkened. Ears were plugged, but not totally sound proofed. No attempt was made to control thought content.

Global Normalization

Change-distribution analysis was applied only after scalar normalization negating global variability, both inter- and intrasubject. Global values (gCBF and gA) were computed as the average of all intracranial pixels (*15*). Every pixel of each scan was then multiplied by a normalization factor, calculated as 50 ml $100g^{-1}$ min^{-1} (laboratory mean gCBF) divided by scan gCBF or as 1,000 counts $pixel^{-1}$ min^{-1} (laboratory mean gA) divided by scan gA.

Intersubject Averaging of Subtraction Images

Intersubject averaging required an anatomically standardized three-dimensional image format. Voxel size was uniform, 2 mm by 2 mm by 2 mm. Each voxel corresponded to a specific anatomic location within the stereotactic coordinate space (*19,22*). The set of coordinate transformations converting primary images into anatomically standardized images were unique for each subject. The required transformations were based on measurements from the lateral skull radiograph (above) and PET-image dimensions (*15,19*).

Image Grouping

Stereotactic-format subtraction images were created for each pair (21 control-minus-control; 28 stimulus-minus-control) of individual rCBF and rA images. These provided the nonaveraged baseline relative to which averaging was tested. Averaged images were formed from groups of 2, 3, 4, 5, 10, 15, and 20 individual subtraction images. Individual images were assigned pseudorandomly into averaging groups using a uniform algorithm. No individual image was included more than once in a given grouping. All individual images were replaced in the selection pool at the start of each grouping (bootstrap procedure with replacement). Ten groups (ten averaged images) were created for each level of averaging.

Region-of-Interest Placement: Local Maximum Algorithm

For regional sampling a subtraction image was considered a finite set of discrete regional changes (independent local maxima) blurred by the limited spatial resolution of PET. A two-stage algorithm was used to identify all members of this set (*23*). The first stage identified all image voxels with a value greater than all adjacent voxels. The second stage estimated the best location of each local maximum with a center-of-mass algorithm operating over a 14-mm-diameter, spherical region of interest. All positive and negative local maxima were identified and recorded by magnitude and location (x, y, z stereotactic coordinates).

Statistical Aanalysis

Each data set consisted of the entire population of independent local maxima within a subtraction image. These populations were characterized by distribution parameters including: the mean, standard deviation, gamma-1 statistic (assessing skew), and gamma-2 statistic (assessing kurtosis).

The gamma-1 statistic (g_1) was computed as,

$$\frac{\Sigma(x - \bar{x})^3}{n\ (s.d.)^3} \quad (1)$$

following Snedecor and Cochran (*24*) where x is the signed magnitude of each member of the distribution either CBF in ml 100 g^{-1} min^{-1} or activity (A) in counts $pixel^{-1}$ min^{-1}; $\bar{x}$, the distribution mean; n, the number of members of the distribution; and s.d., the distribution standard deviation. The g_1 equaled zero for symmetrical populations; positive g_1 indicated a positive skew; negative g_1 indicated a negative skew.

The gamma-2 statistic (g_2) was computed as,

$$\frac{\Sigma(x - \bar{x})^4}{n\ (s.d.)^4} - 3 \quad (2)$$

again following Snedecor and Cochran (*24*). The g_2 was zero for mesokurtotic (normal) populations; leptokurtosis (more outliers than normal) was indicated by positive g_2; platykurtosis (fewer outliers than normal) was indicated by a negative g_2. The presence of significant responses in our stimulus-control distributions was indicated by a positive g_2, i.e., by outliers in the distribution.

As we wished to test independently for positive and negative responses, one-sided g_2 statistics were computed. A one-sided g_2 was simply the g_2 for all values on either side of zero, assuming a population mean ($\bar{x}$) of zero.

TABLE 1
Noise Distribution Parameters

N	N′		Mean	s.d.	Gamma 1	Gamma 2 (two-sided)
1	21	ACTIVITY	−1.48	80.34	−0.06	−0.78
		CBF	−0.07	4.54	−0.04	−0.78
2	10	ACTIVITY	−1.18	50.21	−0.09	−0.74
		CBF	−0.02	2.87	−0.04	−0.77
3	10	ACTIVITY	−1.36	40.00	−0.06	−0.73
		CBF	−0.04	2.281	−0.02	−0.68
4	10	ACTIVITY	−1.38	34.61	−0.09	−0.72
		CBF	−0.02	1.99	−0.02	−0.70
5	10	ACTIVITY	−0.46	30.04	−0.05	−0.67
		CBF	0.02	1.74	−0.02	−0.65
10	10	ACTIVITY	−0.86	19.96	−0.15	−0.54
		CBF	−0.01	1.17	−0.09	−0.64
15	10	ACTIVITY	−1.70	17.24	−0.35	−0.40
		CBF	−0.06	1.01	−0.22	−0.60
20	10	ACTIVITY	−1.39	14.91	−0.32	−0.32
		CBF	−0.06	0.88	−0.21	−0.52

N is the number of individual images per averaged image. N′ is the number of stereotactically averaged images created and searched. The gamma-1 statistic tests skew and is zero for a normal distribution. The gamma-2 statistic tests kurtosis and is zero for a normal distribution, positive for a leptokurtotic distribution (many outliers), and negative for a platykurtotic distribution (few outliners). ACTIVITY indicates regional $H_2{}^{15}O$ (intravenous bolus) tissue-activity data. CBF indicates regional cerebral blood flow values (Kety autoradiographic model).

RESULTS

Image Noise

Noise and the effects of averaging on noise were assessed using control-minus-control subtractions. Noise distributions were symmetric (gamma-1 statistic of 0) about a mean value of zero for both rA and rCBF at all levels of averaging (Table 1, Fig. 2). The distributions were bimodal, an intrinsic property of the local-maximum algorithm (*15*). Bimodality was measured by the gamma-2 statistic as a negative kurtosis ($g_2 < 0$) that lessened with averaging, in accord with the Central Limit Theorum. There were no systematic differences in kurtosis between rA and rCBF (Tables 1,2).

Averaging suppressed image noise equally well for rA and rCBF. The standard deviations of the noise distributions fell as the square of the number of individual subtraction images pooled into each averaged image (Table 1, Fig. 3), in accord with our formulation that the averaged image represents a sampling distribution of means (*15*).

The Physiological Signal

The CBF increase induced in contralateral primary somatosensory cortex by tacticle stimulation (left-hand vibration) was our paradigmatic response, i.e., the signal to be differentiated from background noise (Fig. 1).

Response detection. Sensitivity (1 − false-negative rate) was based on the one-sided g_2 statistic, testing for regional increases (positive one-sided g_2), in CBF as outliers in the distribution of all focal changes in rA or rCBF (Table 2). In individual (nonaveraged) images, sensitivity was 43% and 50% for rA and rCBF, respectively. Sensitivity was 80% for two-image averages for rA and rCBF. Sensitivity was 100% for all averages of 3 or more subtraction images.

Specificity (1 − false-positive rate) also was based on the gamma-2 statistic. Specificity testing independently searched for increases (positive one-sided g_2) and decreases (negative one-sided g_2) in rA and rCBF. No significant outliers (gamma-2 statistic not greater than zero) were found in any images, either individual or averaged. That is, specificity was 100% at all levels of averaging.

Response localization. In stereotactic space, the left hand's primary somatosensory representation fell on the superior aspect of the postcentral gyrus on the lateral convexity of the right hemisphere (*19,22*). Averaging produced no progressive or systematic distortions in response locale (Table 3). The mean absolute difference between rA and rCBF fell steadily with averaging, never exceeding 0.06 cm ("Error" in Table 3). Moreover, in all 98 trials the difference in response locale for matching rA and rCBF images never exceeded 1 pixel (2 mm) in any axis.

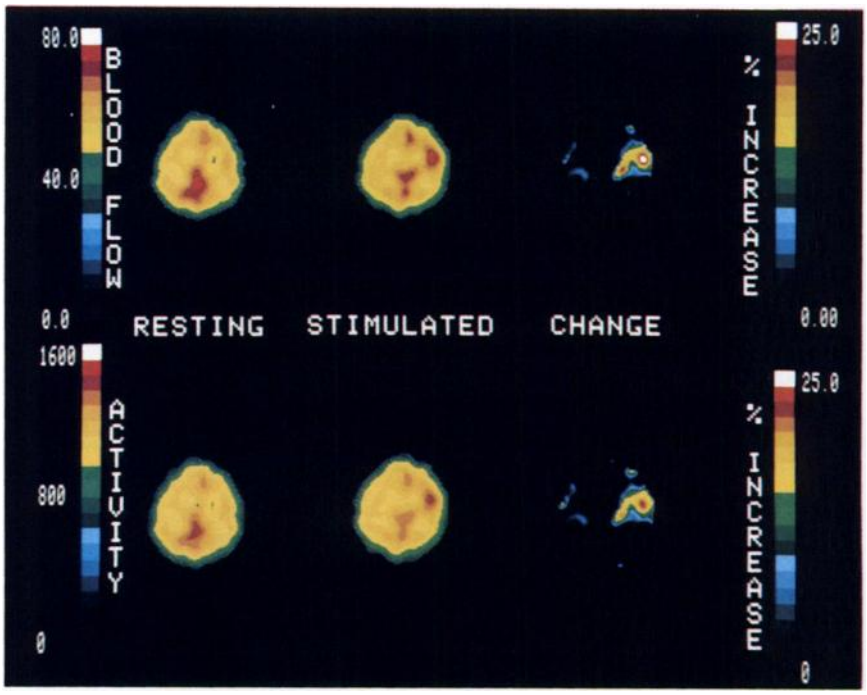

FIGURE 1
PET images of regional blood flow (upper row) and regional tissue activity (lower row) at rest (left column), during left-hand vibration (middle column), and as the percent increase induced by stimulation (right column) are shown for one subject (P944). Bolus, intravenous $H_2{}^{15}O$ was used as a blood flow tracer (40-sec scan duration). Color scales are linear. While the relative regional distributions of blood flow and tissue activity are very similar, blood-flow values in areas of high flow are higher relative to whole-brain mean than tissue activity. For this reason, the percent change in tissue activity slightly underestimates the percent change in blood flow (see text and Table 4).

TABLE 2
Response Detection with the One-Sided Gamma-2 Statistic

N		Stimulus − Control G2+	Sensitivity	Control − Control G2+	G2−	Specificity
1	ACTIVITY	1.2	43% (12/28)	−0.94	−0.95	100% (0/42)
	CBF	1.7	50% (13/28)	−0.91	−0.90	100% (0/42)
2	ACTIVITY	3.5	80% (8/10)	−0.77	−0.88	100% (0/20)
	CBF	4.3	80% (8/10)	−0.79	−0.82	100% (0/20)
3	ACTIVITY	6.5	100% (10/10)	−0.69	−0.84	100% (0/20)
	CBF	7.7	100% (10/10)	−0.67	−0.77	100% (0/20)
4	ACTIVITY	8.8	100% (10/10)	−0.73	−0.76	100% (0/20)
	CBF	10.7	100% (10/10)	−0.74	−0.71	100% (0/20)
5	ACTIVITY	12.4	100% (10/10)	−0.64	−0.75	100% (0/20)
	CBF	12.4	100% (10/10)	−0.66	−0.70	100% (0/20)
10	ACTIVITY	26.6	100% (10/10)	−0.64	−0.49	100% (0/20)
	CBF	28.2	100% (10/10)	−0.71	−0.61	100% (0/20)
15	ACTIVITY	40.31	100% (10/10)	−0.64	−0.30	100% (0/20)
	CBF	39.35	100% (10/10)	−0.72	−0.58	100% (0/20)
20	ACTIVITY	56.8	100% (10/10)	−0.54	−0.21	100% (0/20)
	CBF	54.1	100% (10/10)	−0.63	−0.46	100% (0/20)

N is the number of individual images per averaged image. The gamma-2 statistic tests kurtosis and is zero for a normal distribution, positive for a leptokurtotic (peaked) distribution, and negative for a platykurtotic (flattened) distribution (15). ACTIVITY indicates regional $H_2{}^{15}O$ (intravenous bolus) tissue-activity data. CBF indicates regional cerebral blood flow values (Kety autoradiographic model).

Response magnitude. Response magnitude was computed in 3 ways: simple change in rA or rCBF, percent change, and z-score (Table 4). Simple-change response magnitude fell during averaging, for both rA and rCBF, indicative of residual intersubject variability in response locale (*15*).

Expression of response magnitude in percent change (simple change as a percentage of gCBF or gA) allowed comparison of rA and rCBF. Percent change in rCBF slightly but consistently exceeded that of rA, as expected (Fig. 1) (*15*). As with simple change, percent-change response magnitude fell during averaging.

Expression of response magnitude in z-score (simple change divided by distribution standard deviation) best indicated response significance relative to background image noise, being a signal-to-noise comparison (Fig. 4). Z-scores were virtually identical for rA and rCBF. Averaging increased the mean z-score of the somatosensory response from 4.1 (individual images) to 10.7 (averages of 20 individual images).

DISCUSSION

Functional brain mapping by image-pair subtraction and change-distribution analysis gave results identical in almost all respects for "raw" images of $H_2{}^{15}O$ tissue activity and for processed images of CBF. No loss of response-detection sensitivity or specificity was entailed by the use of tissue-activity images. Response-localization accuracy was as good for rA as for rCBF images. Quantitation of response magnitude by z-score (standard deviations of noise) gave virtually identical values for the two types of data. This equivalence of rA and rCBF held true for both individual images and for stereotactically averaged images.

Advantages

The principal advantages of this less invasive technique for brain mapping are patient safety, comfort, and acceptance of

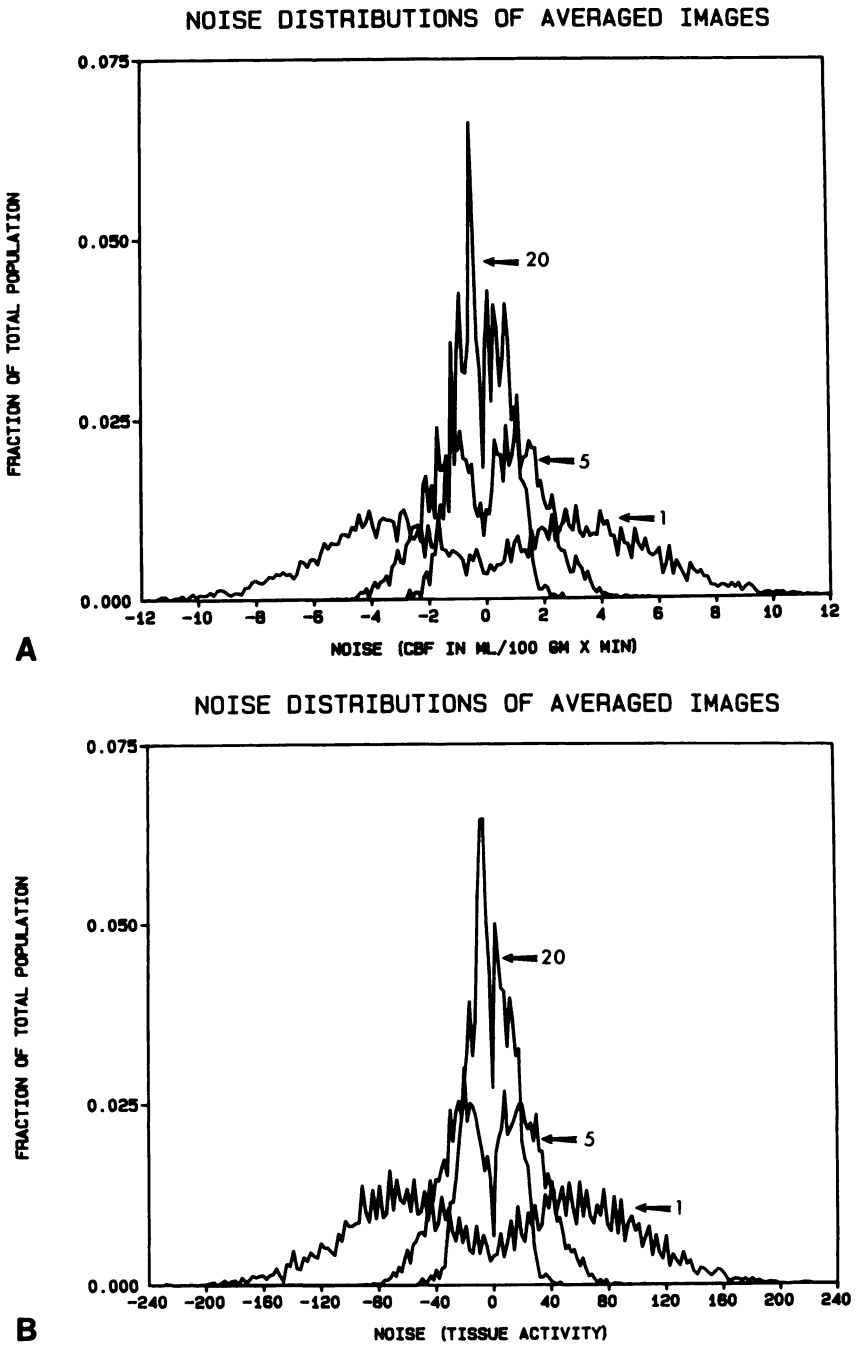

FIGURE 2
Noise-only focal-change distributions are shown for cerebral blood flow (A) and $H_2{}^{15}O$ (intravenous bolus) tissue activity (B). Distributions marked "1" are cumulative from 21 individual, nonaveraged images. Distributions marked "5" and "20" were obtained by stereotactic averaging of 5 and 20 individual images (cumulative distributions for 10 averaged images). Distribution kurtosis and symmetry about zero were identical for blood flow and tissue activity, both individual and averaged (see also Table 1).

the PET procedure. While arterial catheterization is rarely very painful, it is sufficiently unfamiliar, uncomfortable, and anxiety provoking as to be avoided whenever possible. Additionally, during activation studies subjects typically are surrounded by a potentially intimidating array of audiovisual stimulus-delivery equipment and electronic devices monitoring eye movements (EOG), muscle tension (EMG), skin resistance (GSR), and brain electrical activity (EEG). Elimination of the arterial line and blood-drawing technician reduces the complexity of the environment, putting the subject more at ease and improving task performance. Finally, advantages to the investigator are obvious: decreased data processing time, decreased technician cost, and decreased equipment cost.

Limitations

All limitations of noninvasive application of change-distribution analysis pertain to response quantitation in units of CBF.

Whole-brain changes. Global changes in CBF cannot be measured, nor even estimated, without an arterial input function. Thus, when global alterations in CBF are sought, arterial sampling is necessary. For functional mapping, however, global changes are rarely of interest. First, while global CBF and metabolic rate are sensitive to overall level of consciousness (*25*) and to pathological levels of anxiety (*26*), we have not found systematic shifts in global CBF related to task

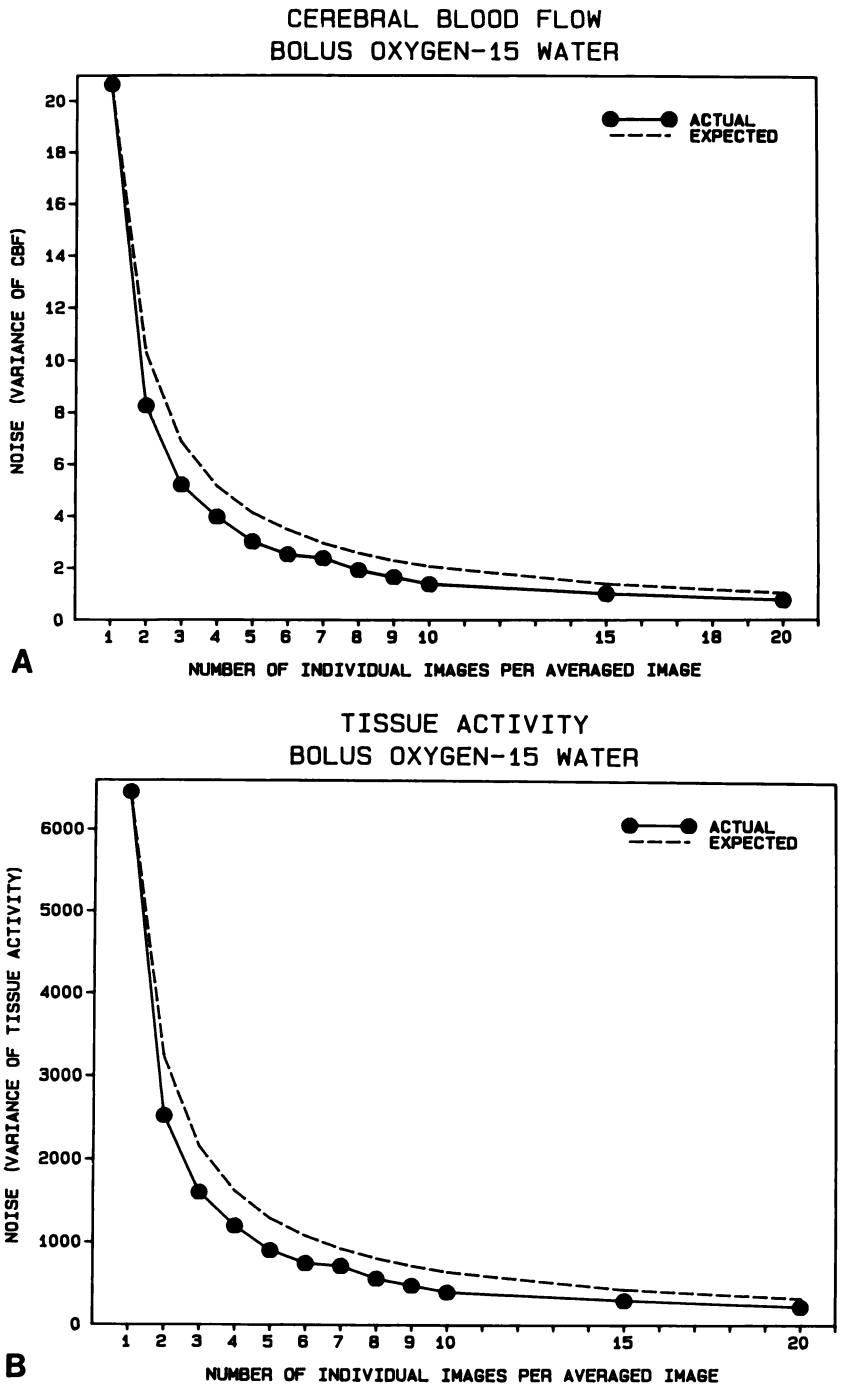

FIGURE 3
Noise was strongly suppressed by image averaging for both blood flow (A) and $H_2{}^{15}O$ (intravenous bolus) tissue activity images (B). The variance of the population of noise (measured in control-minus-control subtractions) varied inversely with the number of images averaged, as predicted by sampling theory. All points represent the mean of ten averaged images with the exception of n = 1, where 21 individual images were sampled.

performance or sensory stimulation (*1-3,13,27*). Second, the relative regional distribution of CBF (i.e., the regional "pattern") is independent of global variations (*28,29*). For this reason, the pattern of regional differences between two images is also independent of global variations. Task-related CBF responses (identified after gCBF normalization) are highly consistent in location and magnitude, both intra- and inter-subject, even in the presence of large fluctuations in gCBF (*1-3,13,27*). Finally, change-distribution analysis specifically seeks regional changes, not global. Global variations confound regional analysis and must be explicitly removed by global normalization.

Response magnitude. Without arterial sampling, response magnitudes cannot be determined in units of CBF (ml 100 g^{-1} min^{-1}). It must be recalled, however, that quantitation of regional CBF change is far from absolute, being strongly influenced by many methodological factors including image resolution, region of interest volume, the local resting CBF, and the level of averaging employed (*15*). Moreover, we identify regional responses only after global normalization. That is, even when expressed in units of CBF, regional changes are properly understood as changes relative to whole-brain mean.

Expressed as percent change relative to whole-brain mean,

TABLE 3
Response Locale

N	N′		Vertical Mean (Error)	Rt-Lt Mean (Error)	AP Mean (Error)
1	28	ACTIVITY	4.9 (0.003)	−4.5 (0.055)	−0.5 (0.020)
		CBF	4.9	−4.4	−0.5
2	10	ACTIVITY	4.9 (0.003)	−4.7 (0.099)	−0.5 (0.020)
		CBF	4.9	−4.8	−0.5
3	10	ACTIVITY	4.8 (0.003)	−4.7 (0.021)	−0.6 (0.019)
		CBF	4.8	−4.7	−0.6
4	10	ACTIVITY	4.9 (0.003)	−4.4 (0.059)	−0.7 (0.020)
		CBF	4.9	−4.3	−0.8
5	10	ACTIVITY	4.9 (0.002)	−4.5 (0.078)	−0.5 (0.002)
		CBF	4.9	−4.5	−0.5
10	10	ACTIVITY	4.8 (0.001)	−4.4 (0.060)	−0.6 (0.039)
		CBF	4.8	−4.5	−0.6
15	10	ACTIVITY	4.9 (0.001)	−4.4 (0.002)	−0.7 (0.000)
		CBF	4.9	−4.4	−0.7
20	10	ACTIVITY	4.8 (0.001)	−4.4 (0.001)	−0.7 (0.001)
		CBF	4.8	−4.4	−0.7

Stereotactic coordinates (expressed in centimeters from the center of the line between the anterior and posterior commissures) for the response of primary somatosensory cortex to left-hand vibration are given. "ACTIVITY" indicates response locations from images of regional $H_2{}^{15}O$ (intravenous bolus) tissue activity. CBF indicates response locations from CBF images. Coordinates for each axis (vertical, right-left, anteroposterior) are given separately. N is the number of individual images per averaged image. N′ is the number of images created at each N. Error (in parentheses) = mean absolute difference in response locale between ACTIVITY and CBF.

regional responses are slightly but consistently greater for rCBF than for rA data. This reflects the slight nonlinearity of the relationship between tissue activity and CBF for the Kety model (*20,21*). The degree of underestimation of rCBF by rA is a function of both the magnitude of the change and the resting regional flow, being greatest for large changes in areas of high flow. For changes of <10%, rA and rCBF response magnitudes are essentially identical (*17*). Moreover, because it is systematic, the effect can be corrected quite effectively. If desired, rCBF percent changes can be computed from rA percent changes to an accuracy of 1–2%, even for very large regional changes (*17*).

Scope of Application

Functional mapping of the normal brain is a cardinal application of noninvasive change-distribution analysis. Identification of the response properties of specific brain regions in normal subjects derives no significant benefit from the use of rCBF rather than rA data. Response location, relative magnitude, and statistical significance can all be determined with equivalent accuracy for rA and rCBF. Intersubject averaging to enhance detection sensitivity is equally effective for rA and rCBF images. Only when global effects are sought is conversion to units of CBF necessary.

Clinical application of these techniques typically will not benefit from arterial catheterization. Preoperative localization of the cortical regions subserving sensorimotor (*3*), linguistic (*4,6*) and other behaviors requires only rA data. In this setting, intrasubject averaging (i.e., averaging multiple scans from a single session) can be used to decrease noise and improve detection of weak responses. Moreover, any analysis based solely on relative regional pattern, such as identification of the zone of interictal hypoflow produced by an epileptic focus, can be accomplished as well with rA as with rCBF images. This allows a single, noninvasive study to achieve two ends: (a) functional mapping, particularly of language-related brain regions; and (b) localization of the epileptogenic lesion. The study of functional responses in cerebrovascular disease is a notable exception to the use of rA data, as hemodynamic status will effect vascular responsiveness and cannot be determined without measurement or regional blood flow, blood volume, oxygen metabolic rate, and oxygen extraction fraction, all of which require arterial sampling (*7,8*).

In conclusion, functional brain mapping using bolus intravenous $H_2{}^{15}O$, image-pair subtraction, change-distribution analysis, and intersubject image averaging is as sensitive and accurate for images of tissue activity as for images of CBF. This makes functional brain mapping extremely safe and simple, requiring only an intravenous catheter and 40 sec, nondynamic scanning. It must be emphasized, however, that we have validated the direct use of tissue-activity images only for functional brain mapping with this specific image-acquisition procedure. The utility of "raw" tissue activity images cannot be assumed for scan durations over 1 min, other methods of $H_2{}^{15}O$ administration (e.g., continuous infusion), other tracers, or applications of PET other than functional brain mapping.

TABLE 4
Response Magnitude

N	N′		Simple Change	Percent Change	Z-Score
1	28	ACTIVITY	316.	32	4.0
		CBF	18.8	38	4.2
2	10	ACTIVITY	250.	25	4.8
		CBF	15.2	30	5.0
3	10	ACTIVITY	250.	25	6.1
		CBF	15.2	30	6.2
4	10	ACTIVITY	230.	23	6.3
		CBF	14.0	28	6.5
5	10	ACTIVITY	218.	22	6.7
		CBF	13.1	26	6.8
10	10	ACTIVITY	219.	22	8.9
		CBF	13.3	27	8.8
15	10	ACTIVITY	211.	21	10.1
		CBF	12.8	26	10.0
20	10	ACTIVITY	211.	21	10.8
		CBF	12.8	26	10.6

Magnitudes of the primary somatosensory cortex response to left-hand vibration are given for cerebral blood flow (CBF) and $H_2{}^{15}O$ (intravenous bolus) tissue activity (ACTIVITY) images. N is the number of individual images per image. N′ is the number of images searched for each N. SIMPLE CHANGE = mean response magnitude for N′ images in ml 100 g^{-1} min^{-1} or counts $pixel^{-1}$ min^{-1} after normalization of whole-brain variation. Percent Change expresses SIMPLE CHANGE as a percent of the whole brain mean. Z-Score = mean SIMPLE CHANGE divided by distribution standard deviation [i.e., signal/(signal + noise)].

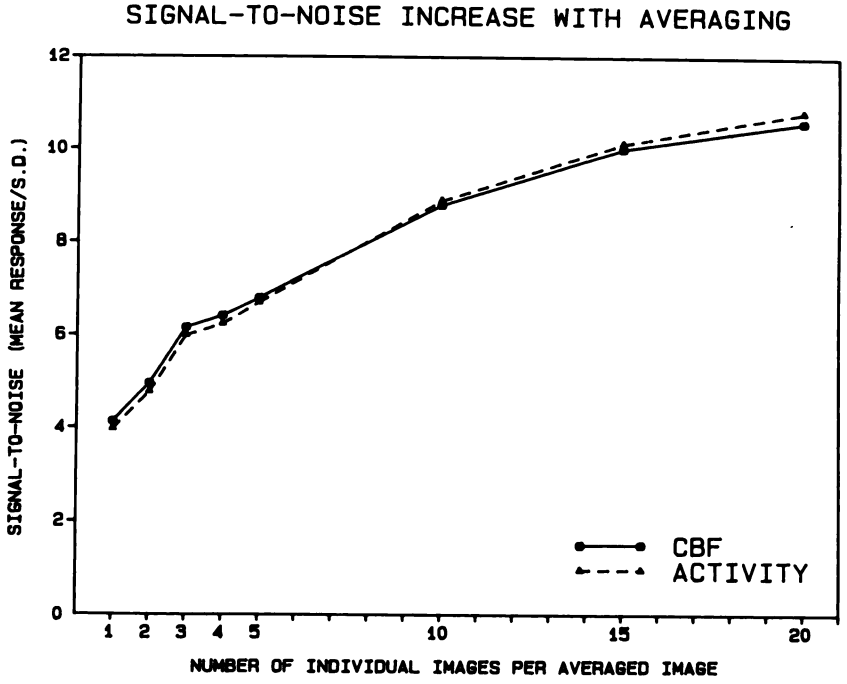

FIGURE 4
Signal-to-noise ratios are plotted for both cerebral blood flow and $H_2{}^{15}O$ (intravenous bolus) tissue activity. N is the number of individual images per averaged image. Signal is the mean magnitude of the primary somatosensory (S1) response at each N (see also, Table 4, simple change). Noise is the standard deviation of the regional change distribution at each N (i.e., noise plus signal).

ACKNOWLEDGMENTS

The authors thank Drs. Marcus Raichle and Michel Ter-Pogossian for providing the intellectual and physical environment in which this work was done. They also thank Lennis Licht, John Hood, Jr., and Thomas Hurley for technical assistance. This work was supported by a grant from the John D. and Catherine T. MacArthur Foundation, and by NIH Grants NS-00904, NS-06833, HL-13851, NS-07025, AG-03991, NS-148344, and MH-00615.

REFERENCES

1. Fox PT, Fox JM, Raichle ME, Burde RM. The role of cerebral cortex in the generation of voluntary saccadic eye movements: a positron emission tomographic study. *J Neurophysiol* 1985; 52:348–368.
2. Fox PT, Miezin ME, Allman JM, Van Essen DC, Raichle ME. Retinotopic organization of human visual cortex mapped with positron emission tomography. *J Neurosci* 1987; 7:913–922.
3. Fox PT, Burton H, Raichle ME. Mapping human somatosensory cortex with positron emission tomography. *J Neurosurg* 1987a; 67:34–43.
4. Petersen SE, Fox PT, Posner MI, Mintun MA, Raichle ME. Positron emission tomographic studies of the cortical anatomy of single-word processing. *Nature* 1988; 331:585–589.
5. Roland PE, Freiberg L. Localization of cortical areas activated by thinking. *J Neurophysiol* 1985; 53:1219–1243.
6. Pardo JV, Fox PT, Goldring S, Raichle ME. Preoperative assessment of cerebral dominance for language using positron emission tomographic measurements of brain blood flow [Abstract]. *Soc Neurosci Abst* 1987; 13:1433.
7. Powers WJ, Fox PT, Raichle ME. The effect of carotid artery disease on the cerebrovascular response to physiological stimulation. *Neurology* 1988; 38:1475–1478.
8. Powers WJ, Fox PT. PET measurements of cerebral blood flow and metabolism: how can they be used to study functional recovery from stroke? In: Ginsberg M, ed. *Cerebrovascular diseases, 16th research (Princeton) conference.* New York: Raven, 1988: in press.
9. Hiess WD. Can PET be used to gauge the brain's capacity for functional recovery from ischemic stroke? In: Ginsberg M, ed. *Cerebrovascular diseases, 16th research (Princeton) conference.* Edited by M. Ginsberg (Raven/New York), 1988: in press.
10. Fox PT, Raichle ME, Mintun MA, Dence C. Nonoxidative glucose consumption during focal physiological neural activity. *Science* 1988; 241:462–464.
11. Raichle ME, Fox PT, Mintun MA. Cerebral blood flow and oxidative glycolysis are uncoupled during somatosensory stimulation in humans [Abstract]. *Soc Neurosci Abst* 1987; 13:812.
12. Ginsberg MD, Change JY, Kelly RE, et al. Increases in both cerebral glucose utilization and blood flow during execution of a somatosensory task. *Ann Neurol* 1988; 23:152–160.
13. Fox PT, Raichle ME. Focal physiological uncoupling of cerebral blood flow and oxidative metabolism during somatosensory stimulation in human subjects. *Proc Natl Acad Sci USA* 1986; 83:1140–1144.
14. Fox PT, Mintun ME, Raichle ME, Miezin FM, Allman JM, Van Essen DC. Mapping human visual cortex with positron emission tomography. *Nature* 1986; 323:806–809.
15. Fox PT, Mintun ME, Reiman EM, Raichle ME. Enhanced detection of focal brain responses using intersubject averaging and change-distribution analysis of subtracted PET images. *J Cereb Blood Flow Metab* 1988; 8:642–653.
16. Herscovitch P, Markham J, Raichle ME. Brain blood

flow measured with intravenous $H_2{}^{15}O$. Theory and error analysis. *J Nucl Med* 1983; 14:782–789.
17. Fox PT, Mintun MA, Raichle ME, Herscovitch P. A noninvasive approach to quantitative functional brain mapping with $H_2{}^{15}O$ and positron emission tomography. *J Cereb Blood Flow Metab* 1984; 4:329–333.
18. Yamamoto M, Ficke D, Ter-Pogossian MM. Performance study of PETT VI, a positron computed emission tomograph with 288 cesium fluoride detectors. *IEEE Trans Nucl Sci* 1982; 29:529–533.
19. Fox PT, Perlmutter JS, Raichle ME. A stereotactic method of anatomical localization for positron emission tomography. *J Comput Assist Tomogr* 1985; 9:141–153.
20. Raichle ME, Martin WRW, Herscotich P, Mintun MA. Markham J. Brain blood flow measured with intravenous $H_2{}^{15}O$. II. Implementation and validation. *J Nucl Med* 1983; 24:790–798.
21. Herscovitch P, Raichle ME, Kilbourn MR, Welch ME. Positron emission tomographic measurement of cerebral blood flow and permeability-surface area product of water using ^{15}O-water and ^{11}C-butanol. *J Cereb Blood Flow Metab* 1987; 7:527–542.
22. Talairach J, Zikla G, Tournoux P, et al. Atlas d'Anatomie Stereotaxique du Telencephale, Masson, Paris, 1967.
23. Mintun MA, Fox PT, Raichle ME. A highly accurate method of localizing regions of neuronal activation in the human brain using positron emission tomography. *J Cereb Blood Flow Metab* 1988: in press.
24. Snedecor GW, Cochran WG. Statistical methods (7th edition). Ames, Iowa: Iowa State University Press, 1982:75–82, 492.
25. Raichle ME. Circulatory and metabolic correlates of brain function in normal humans. In: *Handbook of physiology, the nervous system V*. Bethesda: American Physiological Society, 1987:643–674.
26. Reiman EM, Butler FM, Raichle ME, Herscovitch P, Robins E, Fox PT, and Perlmutter JS. The application of positron emission tomography to the study of panic disorder. *Am J Psychiatr* 1986;143:469–477.
27. Fox PT and Raichle ME. Stimulus rate dependence of regional cerebral blood flow in human striate cortex, demonstrated by positron emission tomography. *J Neurophysiol* 1984; 51:1109–1121.
28. Ball S, Fox PT, Herscovitch P, Raichle ME. Control-state stability for PET brain imaging: "Eyes-closed rest", Same day versus separate day [Abstract]. *Neurology* 1988; 38:363.
29. Ball S, Fox PT, Pardo J, Raichle ME. Control-state stability for PET brain imaging: rest versus task [Abstract]. *Neurology* 1988; 38:363.